AGU PUBLICATIONS

Geophysical Research Letters

RESEARCH LETTER

10.1002/2015GL064944

Key Points:

- Pathway for Atlantic water at 79North unexpectedly found to be via pinned ice front
- Bulk circulation in ice tongue cavities estimated using data
- Renewal timescales for this ice tongue cavity are less than 1 year

Correspondence to:
N. J. Wilson,
nwilson@whoi.edu

Citation:
Wilson, N. J., and F. Straneo (2015), Water exchange between the continental shelf and the cavity beneath Nioghalvfjerdsbræ (79 North Glacier), *Geophys. Res. Lett.*, *42*, 7648–7654, doi:10.1002/2015GL064944.

Received 13 JUN 2015
Accepted 28 JUL 2015
Accepted article online 3 AUG 2015
Published online 22 SEP 2015

Water exchange between the continental shelf and the cavity beneath Nioghalvfjerdsbræ (79 North Glacier)

N. J. Wilson[1,2] and F. Straneo[3]

[1]MIT-WHOI Joint Program in Oceanography/Applied Ocean Science and Engineering, Cambridge, Massachusetts, USA,
[2]Geology and Geophysics Department, Woods Hole Oceanographic Institution, Woods Hole, Massachusetts, USA,
[3]Physical Oceanography Department, Woods Hole Oceanographic Institution, Woods Hole, Massachusetts, USA

Abstract The mass loss at Nioghalvfjerdsbræ is primarily due to rapid submarine melting. Ocean data obtained from beneath the Nioghalvfjerdsbræ ice tongue show that melting is driven by the presence of warm (1°C) Atlantic Intermediate Water (AIW). A sill prevents AIW from entering the cavity from Dijmphna Sund, requiring that it flow into the cavity via bathymetric channels to the south at a pinned ice front. Comparison of water properties from the cavity, Dijmphna Sund, and the continental shelf support this conclusion. Overturning circulation rates inferred from observed melt rates and cavity stratification suggest an exchange flow between the cavity and the continental shelf of 38mSv, sufficient to flush cavity waters in under 1 year. These results place upper bounds on the timescales of external variability that can be transmitted to the glacier via the ice tongue cavity.

1. Introduction

The Northeast Greenland Ice Stream (NEGIS) is a region of rapid ice flow that drains approximately half of the northern sector of the Greenland ice sheet [*Fahnestock et al.*, 2001; *Rignot and Kanagaratnam*, 2006]. Much of the topographical trough NEGIS flows within is below sea level and deepens toward the continental interior [*Bamber et al.*, 2013], suggesting that it could be susceptible to marine ice sheet instability [*Weertman*, 1974]. The buttressing effect of ice tongues at outlet glaciers provides a stabilizing influence on marine ice sheets [*Dupont and Alley*, 2005]. The inferred presence of the ice tongue Nioghalvfjerdsbræ (79NG) at the terminus of NEGIS over the past 4ka [*Reeh et al.*, 2001] suggests it to be stable, although it has advanced and retreated many tens of kilometers since the early Holocene [*Reeh et al.*, 2001; *Evans et al.*, 2009]. In contrast, neighboring Zachariæ Isstrøm (ZI), the second marine outlet of NEGIS, has experienced collapse and rapid retreat since 2002 [*Rignot and Kanagaratnam*, 2006; *Khan et al.*, 2014] indicating that the region may be undergoing change. Because of the large area drained by NEGIS and the potential for large sea level rise if it should become unstable in the future, it is important to assess the likelihood of future retreat.

79NG terminates with a 70km long and 20km wide ice tongue that floats in Nioghalvfjerdsfjorden and has a grounding depth of 600m [*Mayer et al.*, 2000]. 79NG is noteworthy in that the majority of mass loss is driven by melting at the ice-ocean interface at the base of the ice tongue, rather than by calving [*Reeh et al.*, 1999]. The most rapid melting occurs in the vicinity of the grounding zone [*Seroussi et al.*, 2011], where the ice tongue is thickest and exposed to deeper and warmer waters. Increases in submarine melt rates could lead to thinning, resulting in a reduction in buttressing capacity and loss of ice shelf strength. A similar sequence of events is believed to have driven the recent acceleration and retreat of Jakobshavn Isbræ in western Greenland [*Holland et al.*, 2008; *Motyka et al.*, 2011]. The loss of buttressing provided by the former Larsen B ice shelf in Antarctica also led to outlet glacier acceleration [*Scambos et al.*, 2004; *Rignot et al.*, 2004]. To assess the stability of 79NG and NEGIS to changes in ocean forcing, we first need to understand the present state of ice-ocean interactions. This includes identifying the circulating water masses, the pathways through which they enter the cavity, and the processes that govern their variability.

79NG abuts Hovgaard Ø, which divides the ice tongue into two sections (Figure 1a). As a result, two potential pathways for water flow into the 79NG cavity exist. One, bypassing Hovgaard Ø to the north through the 80km long Dijmphna Sund, provides access to a northern terminus from Westwind Trough on the continental shelf. Alternatively, water may flow beneath a bathymetrically pinned ice front south of Hovgaard Ø that potentially links the cavity to warm waters that reside in Norske Trough to the south. On the shelf, shallow Polar

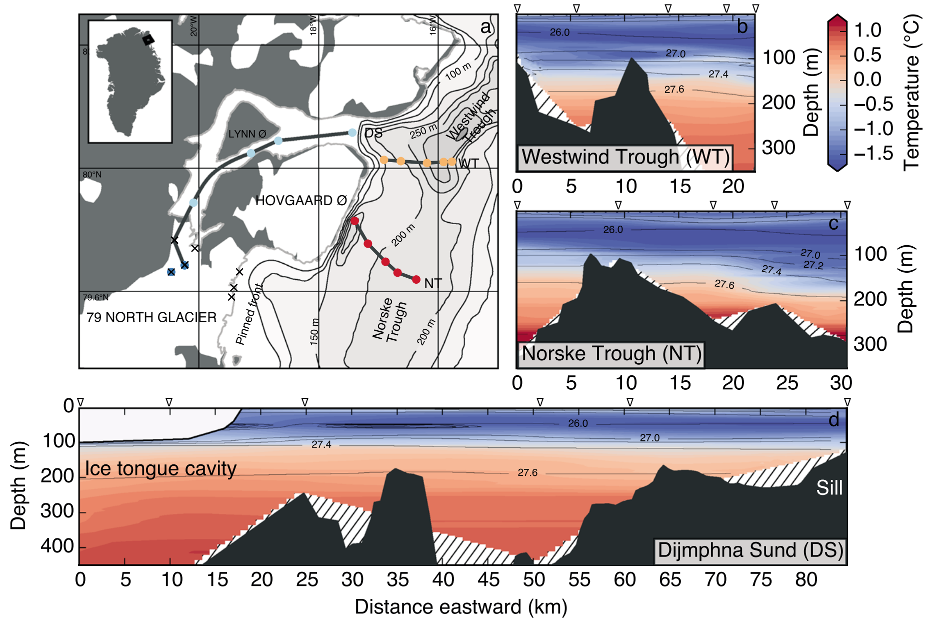

Figure 1. (a) Region map with selected sections of potential temperature (color) and density (contours) for (b) Westwind Trough ("WT"), (c) Norske Trough ("NT"), and (d) Dijmphna Sund ("DS"). Map dots indicate salinity, temperature, and depth (CTD) profile locations, and crosses indicate expendable bathythermograph (XBT) profile locations. Sections are plotted from west to east, i.e., looking northward. International Bathymetric Chart of the Arctic Ocean bathymetry shown in Figure 1a is inaccurate near glacier and within Dijmphna Sund.

Water (PW) circulates counterclockwise through Norske Trough and Westwind Trough around Belgica Bank [*Schneider and Budéus*, 1995; *Johnson and Niebauer*, 1995; *Topp and Johnson*, 1997]. Circulation of deeper and warmer Atlantic Intermediate Water (AIW) is less clearly defined. Previous surveys have found the warmest waters to be confined to Belgica Trough and Norske Trough and apparently distinct from the AIW found in Westwind Trough [*Budéus et al.*, 1997]. *Mayer et al.* [2000] propose that AIW originating in Westwind Trough enters the cavity by flowing through Dijmphna Sund. In this scenario, Westwind Trough is the primary source of AIW interacting with the glacier.

We present data collected in 2009 that indicates that the main pathway for AIW into the cavity is beneath the pinned ice front instead. The significance of this result is that cavity exchange with warmer water masses in Norske Trough is possible. This constitutes a more direct route, and one that is likely strongly influenced by the distribution of sea ice near the pinned front and by mixing processes within bathymetric channels beneath the pinned front. Our measurements also indicate that some of the relatively fresh glacially modified water is exported to the continental shelf via Dijmphna Sund. Finally, we use water properties measured from the 79NG cavity in combination with a simple model of an overturning circulation to show that the renewal of water within the cavity occurs on timescales of less than 1 year, requiring a fairly vigorous exchange between the continental shelf and the cavity.

2. Data

In September 2009, salinity, temperature, and depth (CTD) surveys in Dijmphna Sund and west of Belgica Bank were conducted from the icebreaker M/V *Arctic Sunrise* over the course of 4 days with an RBR XR-620 profiler (Figure 1a). Thick landfast ice limited the spatial extent of sampling. Bathymetry was collected along the ship track using a single beam depth sounder.

On the continental shelf, we surveyed two east-west sections that we refer to as Westwind Trough (north) and Norske Trough (south) after the two deep bathymetric troughs nearby (Figure 1a). We also measured properties along a section through Dijmphna Sund, including cross-fjord sections at the fjord mouth and near the glacier terminus. Sea ice prevented the collection of profiles near the pinned terminus. Two additional CTD profiles, 5km apart, were collected via helicopter in a rift in the floating ice tongue, 15km upglacier from the northern terminus. These profiles provide a snapshot of properties within 79NG's cavity. In addition to the

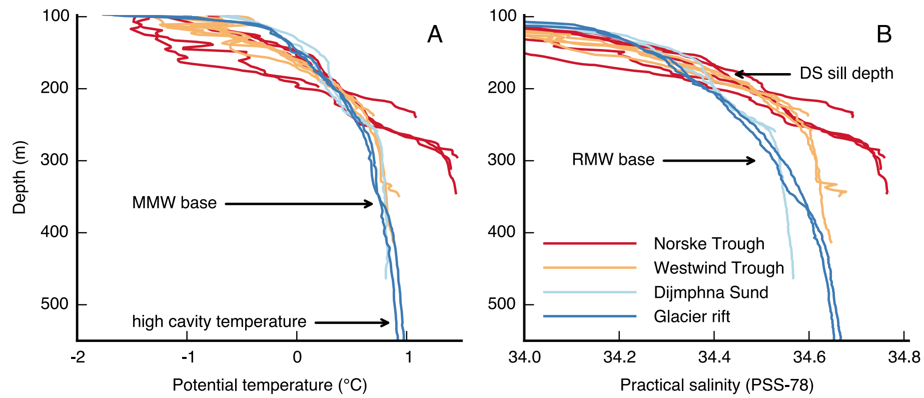

Figure 2. (a) Potential temperature and (b) practical salinity for casts from Norske Trough (NT), Westwind Trough (WT), Dijmphna Sund (DS), and the glacier cavity. See text for discussion.

CTD profiles described above, a number of Sippican T-5, T-6, and T-7 expendable bathythermograph (XBT) profiles were collected by helicopter survey from the rift, northern terminus, and pinned ice front (Figure 1a).

3. Results

3.1. Shelf Properties

Regionally, we observe relatively warm AIW ($\theta > 0°$C; $S > 34.3$) at depth, while colder and fresher PW occupies the upper 100–150m (Figures 1b and 1c), in agreement with prior surveys [e.g., *Bourke et al.*, 1987; *Budéus and Schneider*, 1995]. The warmest waters were observed in Norske Trough immediately east of Hovgaard Ø. We find these waters to be distinct from the warmest waters in Westwind Trough to the north. As indicated by the large contrast in temperature (0.6°C) and salinity (0.13) (Figure 2), as well as the overlap in temperature-salinity space (Figure 3), a barrier may separate the two troughs, preventing the warmer and denser Norske Trough water from moving northward. Sea ice cover prevented us from mapping the bathymetry in this region. The lower temperatures in Westwind Trough relative to Norske Trough match similar observations reported by *Budéus and Schneider* [1995]. In measurements described by *Mayer et al.* [2000], a warm layer is reported near the pinned front, similar to our findings in Norske Trough.

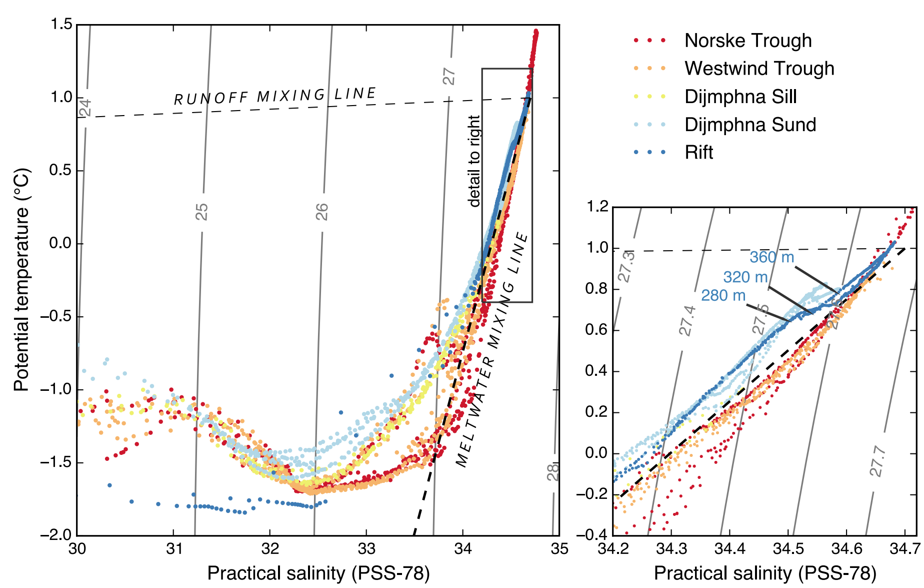

Figure 3. Potential temperature and practical salinity plots from all stations. The dashed meltwater and runoff mixing lines connect a hypothetical ambient water (S = 34.75, T = 1.0°C) to water derived from melting ice in contact with the ocean and runoff derived from melting away from the ocean, respectively. (left) Overview of including the bulk of the water column. (right) Expanded view representing the deepest water masses. Depths in the rift casts annotated for reference to the text.

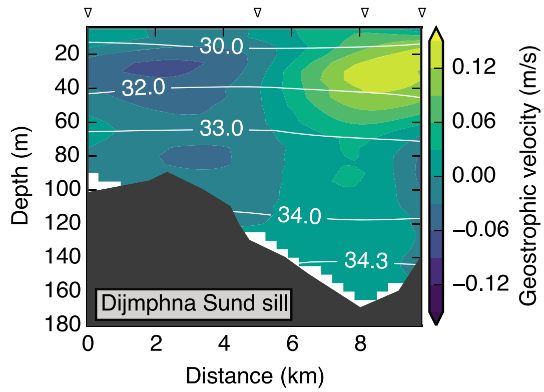

Figure 4. Geostrophic velocity calculated across the Dijmphna Sund mouth (shown from south to north), with flow assumed zero at the bottom as a reference. Contours are salinity (note irregular intervals).

3.2. Inflow Pathways

At the mouth of Dijmphna Sund, we mapped a shallow sill blocking inflow of AIW from the continental shelf (Figure 4). This sill has been followed across the channel and has a maximum depth of ≈170m. That the sill is an obstacle to the flow of AIW from the continental shelf to the cavity is confirmed by a large salinity contrast (0.1) observed between Dijmphna Sund and the deep waters below 180m on the continental shelf (Figure 2). These findings suggest that the deep (greater than 200m) waters in Dijmphna Sund are not primarily due to flow over the sill, contradicting the conclusions by *Mayer et al.* [2000]. We turn to the alternative possibility that AIW primarily flows to the glacier beneath the pinned front, filling Dijmphna Sund from near the glacier terminus.

Sub-ice shelf properties sampled from the glacial rift southwest of Dijmphna Sund broadly mimic those on the continental shelf, insomuch as deeper water is warmer and saltier. The deepest waters bear closest resemblance to those in Norske Trough (Figure 3, inset). Maximum temperatures from the rift exceed maximum water temperatures in Westwind Trough (by 0.2°C) and Dijmphna Sund (by 0.25°C) (Figure 2). This finding further supports our conclusion that the AIW flowing into the glacier cavity originates from Norske Trough and flows into the cavity under the pinned front. Soundings collected by *Mayer et al.* [2000] show a seabed topography near the glacier front exceeding 300m depth, allowing such a pathway. Finally, the differences in properties between the cavity and Dijmphna Sund below 350m suggests that there could be an additional sill separating the cavity under the ice from the deep Dijmphna Sund basin (Figure 2).

3.3. Glacial Modification and Export Pathways

By analyzing the temperature and salinity of different water masses [e.g., *Straneo et al.*, 2012], we infer the presence in the cavity of both glacial meltwater-modified water (MMW) and glacial runoff-modified water (RMW), formed by mixing between ambient ocean water and meltwater formed upstream of the grounding zone, such as surface melt. MMW is identified on the basis of T-S anomalies along the meltwater line (Figure 3) relative to the trend observed on the continental shelf. On the other hand, RMW water is fresher than the water from which it derives and therefore plots to the left of the continental shelf water masses in T-S space.

We observe MMW above ~360m depth, while RMW exists above ~300m depth. The MMW signature is clearest in when collapsed onto a temperature versus depth plot (Figure 2a), where water above 360m is 0.2–0.3°C colder than water below. Because the temperature shift is apparent in many deep CTD and XBT profiles from the rift and northern terminus, we believe that the hypothesized MMW-modified layer is widely distributed in space. A thick (>300m) layer of MMW-modified water has been described at Petermann Fjord in northwestern Greenland by *Johnson et al.* [2011], and our data are consistent with a similarly modified layer here. The glacial runoff signature manifests as an offset in T-S space near the 27.6kgm^{-3} isopycnal (Figure 3, inset). Water in the rift at this depth is fresher than the water below without a corresponding temperature change characteristic of MMW. It would be possible to form a similar water mass by modification of dense Norske Trough water not observed in the cavity; however, the absence of any intermediate water masses resulting from mixing suggests instead that the relatively fresh water derives from injection of runoff into the cavity.

At the head of Dijmphna Sund, water is fresher than found on the continental shelf (see Dijmphna Sund data in Figure 3). The salinity anomaly weakens toward the sill consistent with mixing with shelf water. The low salinity indicates mixing with freshwater, while the along fjord gradient suggests that the source is RMW and that the northern terminus is one pathway by which modified water leaves the cavity. At the same time, the upper PW layer is warmer near the glacier than near the sill (Figure 1d). A similar pattern has been observed by *Straneo et al.* [2012] in other Greenland fjord systems characterized by increasing temperature with depth and diagnosed as upwelling of warmer and deeper water freshened through glacial modification. At the mouth of Dijmphna Sund, a geostrophically inferred flow implies laterally varying exchange (Figure 4). A plume from

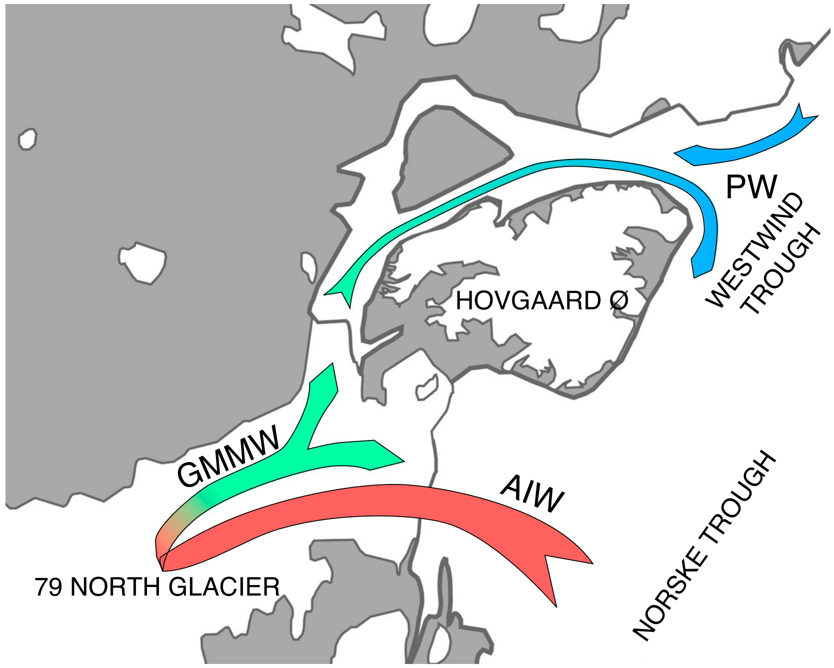

Figure 5. Schematic illustration of inferred pathways for AIW (red), PW (blue), and MMW (green). Heat enters the 79NG cavity from Norske Trough via the pinned front because a sill at Dijmphna Sund excludes AIW from Westwind Trough. Mixing between modified AIW (MMW) and PW takes place in Dijmphna Sund.

the Dijmphna Sund mouth may contribute to a low salinity anomaly on the continental shelf east of Hovgaard Ø at depths shallower than 100m.

3.4. Cavity Circulation

Within the cavity, the vertical distribution of unmodified and glacially modified water types suggests that warm AIW enters at depth, driving melting and mixing with glacial runoff. The less dense modified waters formed by mixing during this interaction rise and spread beneath the ice tongue (Figure 5). The net circulation therefore involves a net inflow at depth and a net outflow of MMW and RMW within the upper portion of the water column, similar to the net circulation expected to take place in other glacial fjords [e.g., *Motyka et al.*, 2003; *Johnson et al.*, 2011; *Sutherland et al.*, 2014].

Previous researchers have applied various salt balance techniques to estimate rates of estuarine overturning in glacial fjords [e.g., *Straneo et al.*, 2010; *Sutherland et al.*, 2014]. Such approaches are limited in particular by the uncertain freshwater input into the fjord from melting and runoff. Instead, we employ a thermal analog to the Knudsen conservation relation for estuarine circulation to place bounds on the net exchange flow. In common with previous methods we assume a two-layer exchange driven by freshening due to glacial inputs; however, our approach only requires knowledge of the submarine melt rate. For glaciers with floating ice, the submarine melt rate can be estimated via ice flux divergence methods [e.g., *Seroussi et al.*, 2011]. We neglect temporal variability, which is discussed further below.

The cavity heat budget is simplified due to the fact that it is completely enclosed by the ice tongue and fjord bathymetry everywhere except at the mouth. Given that the heat budget within the cavity is controlled by water advection at the mouth and latent heat costs for melting ice, the simple relation holds

$$Q_e = \frac{L_f}{c_w}\left(\frac{Q_m}{T_{in} - T_{out}}\right), \quad (1)$$

where Q_e is the overturning exchange flow implied at the cavity mouth, Q_m is the flux of meltwater, L_f is the latent heat of fusion, c_w is the specific heat for water, and T_{in} and T_{out} are the potential temperatures of incoming and outgoing water, respectively. This relation neglects vertically averaged flow terms at the mouth as well as the effect of glacial runoff entering the cavity, both of which are small.

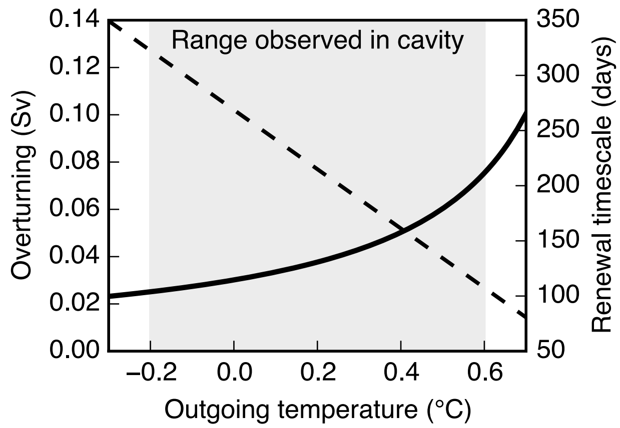

Figure 6. Fjord inflow (solid) and renewal timescale (dashed) predicted as a function of outflow temperature using inflow temperature constrained by measurements and melt rates estimated by *Mayer et al.* [2000]. The region of likely outflow temperature is shaded.

Mayer et al. [2000] report annual melt volumes of ∼11.2km^3 yr^{-1} based on flux divergence, requiring ∼3.7 × 10^{18} Jyr^{-1} of heat input. Assuming that the inflowing water is the deepest because it is denser prior to glacial modification, we estimate T_{in} ≈1°C (Figure 2a). Our measurements indicate that possible values for the glacially modified outgoing water are in the range −0.2°C ≤ T_{out} ≤ 0.6°C. The resulting exchange flows, using the published melt rate estimate, are shown in Figure 6. Selecting an outgoing water temperature of 0.2°C, which is roughly in the middle of the range of modified waters in the cavity (Figure 2a), the exchange flow at the cavity mouth is 38mSv, compared to 0.36mSv of meltwater flux. Given a mean water column thickness of 500m and cavity dimensions of 70km by 20km, the estuarine timescale is ∼215days. This timescale is a maximum estimate of a cavity exchange timescale, as other processes may also contribute to exchange [e.g., *Straneo et al.*, 2010]. Over the range of plausible values for outgoing temperature suggested above, the estuarine timescale ranges from 110 to 320days.

Temporal variability in the incoming water temperature is unknown, and our ability to estimate the overturning flow depends on the relative timescales of external variability and fjord renewal. The estimate above is based on an assumption that the temperature stratification observed in the cavity is representative of values over longer periods. Also, the inferred melt rates represent time-averaged values that may not be representative of current water temperatures and properties.

4. Discussion and Summary

Observed bathymetry and water properties show that AIW does not primarily enter the 79NG cavity from Dijmphna Sund, as hypothesized by *Mayer et al.* [2000]. This statement is supported by two lines of evidence. On the continental shelf, AIW with temperature greater than 1°C occurs in our data only at 230–270m (Figure 2), well below the depth of the sill in Dijmphna Sund. Second, maximum temperatures in the cavity are greater than temperatures observed in Dijmphna Sund, further indicating that AIW beneath the ice tongue does not transit through Dijmphna Sund. The nature of the survey does not permit us to put the observed spatial variability into the context of temporal variability. However, the salinity contrast below 170m depth observed on either side of the sill confirms that the sill is an effective barrier to the exchange of deeper waters. In addition, density calculated in the rift below 350m is higher than that in Dijmphna Sund. This suggests that there could be a second sill separating Dijmphna Sund from the rift. Measurements taken from Dijmphna Sund are therefore unlikely to be representative of the 79NG cavity, and it appears that the deepest waters in Dijmphna Sund are isolated from both Westwind Trough and the cavity. The remaining alternative pathway for AIW is renewal via the pinned ice front. *Mayer et al.* [2000] describe bathymetric data that support the existence of deep (∼400m) channels beneath the pinned front. Inflow of AIW into the cavity is therefore likely to occur through such deep channels. Given the limited nature of the survey, it was impossible to assess the extent to which seasonal or higher frequency fluctuations in the PW-AIW interface depth might affect the exchange between the continental shelf and the ice shelf cavity. A better understanding of temporal variability in the front between PW and AIW on the continental shelf is important for characterizing the potential for warmer water to enter the cavity in past and future climates.

The conclusion that the transport of warm water to the 79NG cavity does not directly involve Dijmphna Sund has implications for the effect on the glacier of variability on the continental shelf. The pinned terminus also appears to provide a shorter pathway between the shelf and the cavity, exposing the cavity more directly to the impact of shelf-driven processes such as intermediary flows [e.g., *Jackson et al.*, 2014]. The near perennial, extensive sea ice barrier just beyond the terminus could also have an impact on the access of AIW to the cavity. If the recent initiation of quasi-seasonal disintegration of the Norske Øer Ice Barrier [*Hughes et al.*, 2011] changes the dynamics of local currents and the Northeast Water Polynya, then the supply of warm water into the glacier cavity could be altered.

Melting beneath 79NG results in formation of MMW, which mixes with ambient AIW to form glacially modified water observed in the cavity and Dijmphna Sund. Also present is a signature from mixing with glacial runoff. The resulting glacially modified waters are less dense than the ambient water, resulting in a shallow layer of anomalously warm water and an overturning exchange circulation that drives heat flow into the cavity and is driven by glacial melting.

Based on an idealized model of an overturning circulation with heat conservation, we estimate the exchange between the cavity and the continental shelf associated with melting to be ∼40mSv. An exchange flow of this magnitude implies timescales of water renewal of less than 1 year and underscores the highly coupled nature of ice-ocean interactions. This is relevant to both discussions of past and future ocean-forced variability at 79NG. Additional data are required to evaluate the role played by other external mechanisms in cavity renewal. Further mapping of the channels and measurement of the daily to interannual variability in shelf and cavity processes are critical future steps in assessing the sensitivity of 79NG to ocean processes.

Acknowledgments
We would like to acknowledge assistance from the crew of the M/V *Arctic Sunrise* and Greenpeace International Inc., as well as help obtained during and subsequent to field work from Dave Sutherland, Gordon Hamilton, and Leigh Stearns. Crucial funding came from WHOI's Ocean and Climate Change Institute, NASA grant NNX13AK88G, and NSF grant OCE-1434041. The data collected for this research may be obtained by contacting the authors.

The Editor thanks two anonymous reviewers for their assistance in evaluating this paper.

References

Bamber, J., et al. (2013), A new bed elevation dataset for Greenland, *Cryosphere*, *7*(2), 499–510.

Bourke, R. H., J. L. Newton, R. G. Paquette, and M. D. Tunnicliffe (1987), Circulation and water masses of the East Greenland Shelf, *J. Geophys. Res.*, *92*(C7), 6729–6740.

Budéus, G., and W. Schneider (1995), On the hydrography of the Northeast Water Polynya, *J. Geophys. Res.*, *100*(C3), 4287–4299.

Budéus, G., W. Schneider, and G. Kattner (1997), Distribution and exchange of water masses in the Northeast Water Polynya (Greenland Sea), *J. Mar. Syst.*, *10*(1), 123–138.

Dupont, T. K., and R. B. Alley (2005), Assessment of the importance of ice-shelf buttressing to ice-sheet flow, *Geophys. Res. Lett.*, *32*, L04503, doi:10.1029/2004GL022024.

Evans, J., C. Ó Cofaigh, J. A. Dowdeswell, and P. Wadhams (2009), Marine geophysical evidence for former expansion and flow of the Greenland ice sheet across the north-east Greenland continental shelf, *J. Quat. Sci.*, *24*(3), 279–293.

Fahnestock, M., I. Joughin, T. Scambos, R. Kwok, W. Krabill, and S. Gogineni (2001), Ice-stream-related patterns of ice flow in the interior of northeast Greenland, *J. Geophys. Res.*, *106*(D24), 34,035–34,045.

Holland, D. M., R. H. Thomas, B. De Young, M. H. Ribergaard, and B. Lyberth (2008), Acceleration of Jakobshavn Isbræ triggered by warm subsurface ocean waters, *Nat. Geosci.*, *1*, 659–664, doi:10.1038/ngeo316.

Hughes, N. E., J. P. Wilkinson, and P. Wadhams (2011), Multi-satellite sensor analysis of fast-ice development in the Norske øer Ice Barrier, northeast Greenland, *Ann. Glaciol.*, *52*(57), 151–160.

Jackson, R. H., F. Straneo, and D. A. Sutherland (2014), Externally forced fluctuations in ocean temperature at Greenland glaciers in non-summer months, *Nat. Geosci.*, *7*, 503–508, doi:10.1038/ngeo2186.

Johnson, H. L., A. Münchow, K. K. Falkner, and H. Melling (2011), Ocean circulation and properties in Petermann Fjord, Greenland, *J. Geophys. Res.*, *116*, C01003, doi:10.1029/2010JC006519.

Johnson, M., and H. J. Niebauer (1995), The 1992 summer circulation in the Northeast Water Polynya from acoustic Doppler current profiler measurements, *J. Geophys. Res.*, *100*(C3), 4301–4307.

Khan, S. A., et al. (2014), Sustained mass loss of the northeast Greenland ice sheet triggered by regional warming, *Nat. Clim. Change*, *4*, 292–299.

Mayer, C., N. Reeh, F. Jung-Rothenhäusler, P. Huybrechts, and H. Oerter (2000), The subglacial cavity and implied dynamics under Nioghalvfjerdsfjorden Glacier, NE-Greenland, *Geophys. Res. Lett.*, *27*(15), 2289–2292, doi:10.1029/2000GL011514.

Motyka, R. J., L. Hunter, K. A. Echelmeyer, and C. Connor (2003), Submarine melting at the terminus of a temperate tidewater glacier, LeConte Glacier, Alaska, USA, *Ann. Glaciol.*, *36*(1), 57–65.

Motyka, R. J., M. Truffer, M. Fahnestock, J. Mortensen, S. Rysgaard, and I. Howat (2011), Submarine melting of the 1985 Jakobshavn Isbræ floating tongue and the triggering of the current retreat, *J. Geophys. Res.*, *116*, F01007, doi:10.1029/2009JF001632.

Reeh, N., C. Mayer, H. Miller, H. H. Thomsen, and A. Weidick (1999), Present and past climate control on fjord glaciations in Greenland: Implications for IRD-deposition in the sea, *Geophys. Res. Lett.*, *26*(8), 1039–1042.

Reeh, N., H. H. Thomsen, A. K. Higgins, and A. Weidick (2001), Sea ice and the stability of north and northeast Greenland floating glaciers, *Ann. Glaciol.*, *33*, 474–480.

Rignot, E., and P. Kanagaratnam (2006), Changes in the velocity structure of the Greenland ice sheet, *Science*, *311*(5763), 986–990.

Rignot, E., G. Casassa, P. Gogineni, W. Krabill, A. Rivera, and R. Thomas (2004), Accelerated ice discharge from the Antarctic Peninsula following the collapse of Larsen B ice shelf, *Geophys. Res. Lett.*, *31*, L18401, doi:10.1029/2004GL020697.

Scambos, T. A., J. A. Bohlander, C. A. Shuman, and P. Skvarca (2004), Glacier acceleration and thinning after ice shelf collapse in the Larsen B embayment, Antarctica, *Geophys. Res. Lett.*, *31*, L18402, doi:10.1029/2004GL020670.

Schneider, W., and G. Budéus (1995), On the generation of the Northeast Water Polynya, *J. Geophys. Res.*, *100*(C3), 4269–4286.

Seroussi, H., M. Morlighem, E. Rignot, E. Larour, D. Aubry, H. B. Dhia, and S. S. Kristensen (2011), Ice flux divergence anomalies on 79North Glacier, Greenland, *Geophys. Res. Lett.*, *38*, L09501, doi:10.1029/2011GL047338.

Straneo, F., G. S. Hamilton, D. A. Sutherland, L. A. Stearns, F. Davidson, M. O. Hammill, G. B. Stenson, and A. Rosing-Asvid (2010), Rapid circulation of warm subtropical waters in a major glacial fjord in East Greenland, *Nat. Geosci.*, *3*(3), 182–186.

Straneo, F., D. A. Sutherland, D. Holland, C. Gladish, G. S. Hamilton, H. L. Johnson, E. Rignot, Y. Xu, and M. Koppes (2012), Characteristics of ocean waters reaching Greenland's glaciers, *Ann. Glaciol.*, *53*(60), 202–210.

Sutherland, D. A., F. Straneo, and R. S. Pickart (2014), Characteristics and dynamics of two major Greenland glacial fjords, *J. Geophys. Res. Oceans*, *119*, 3767–3791, doi:10.1002/2013JC009786.

Topp, R., and M. Johnson (1997), Winter intensification and water mass evolution from yearlong current meters in the Northeast Water Polynya, *J. Mar. Syst.*, *10*(1), 157–173.

Weertman, J. (1974), Stability of the junction of an ice sheet and an ice shelf, *J. Glaciol.*, *13*, 3–11.